Published in final edited form as:
J Morphol. 2003 July ; 257(1): 33. doi:10.1002/jmor.10104.

Biomechanics of the Rostrum and the Role of Facial Sutures

Katherine L. Rafferty[*], **Susan W. Herring**, and **Christopher D. Marshall**
Department of Orthodontics, University of Washington, Seattle, Washington 98195

Abstract

The rostrum is a large diameter, thin-walled tubular structure that receives loads from the teeth. The rostrum can be conceptualized both as a rigid structure and as an assemblage of several bones that interface at sutures. Using miniature pigs, we measured in vivo strains in rostral bones and sutures to gain a better understanding of how the rostrum behaves biomechanically. Strains in the premaxillary and nasal bones were low but the adjacent maxillary-premaxillary, internasal, and intermaxillary suture strains were larger by an order of magnitude. While this finding emphasizes the composite nature of the rostrum, we also found evidence in the maxillary and nasal bones for rigid structural behavior. Namely, maxillary strain is consistent with a short beam model under shear deformation from molar loading. Strain in the nasal bones is only partially supported by a long beam model; rather, a complex pattern of dorsal bending of the rostrum from incisor contact and lateral compression is suggested. Torsion of the maxilla is ruled out due to the bilateral occlusion of pigs and the similar working and balancing side strains, although it may be important in mammals with a unilateral bite. Torsional loading does appear important in the premaxillae, which demonstrate working and balancing side changes in strain orientation. These differences are attributed to asymmetrical incisor contact occurring at the end of the power stroke.

Keywords

craniofacial suture; pig; facial bones; bone strain

Compared to the mandible, fewer attempts have been made to model or measure the in vivo loading of the upper jaw. There are a number of interesting contrasts in both the sources of loading in these two elements and in their design. The muscles attaching to the mandible generate forces that are opposed by reaction forces at the teeth and jaw joints. In animals with fused symphyses, such as pigs and higher primates, the mandible can be modeled as a rigid curved beam (Demes et al., 1984; Wolff, 1984; Hylander, 1985; van Eijden, 2000). In primates, the loads imposed by muscle and reaction forces cause complex patterns of stress and strain in the mandible, including sagittal and transverse bending and deformation from shear and torsion (Hylander, 1979, 1984; Demes et al., 1984; Wolff, 1984; Hylander and Johnson, 1994). In contrast, the maxillary and premaxillary bones receive loads primarily from forces generated by occlusion with the mandibular teeth. Except for a small portion of the masseter, the muscles do not attach directly to the bones of the upper jaw. An added complication is that, unlike the single rigid structure of the mandible, the bones of the rostrum (maxillae, premaxillae, and nasals) are connected to one another via sutures, which generally remain patent until late in life (longer than braincase sutures). The mechanical properties of the sutures

*Correspondence to: Katherine Rafferty, Department of Orthodontics, Box 357446, University of Washington, Seattle, WA 98195. kraff@u.washington.edu.
Current address for C. Marshall: Department of Marine Biology, Texas A&M at Galveston, Galveston, TX 77551.

and bones differ from one another (Jaslow, 1990), creating a composite structure in which energy is disproportionately absorbed through sutural deformation.

Nevertheless, idealized rigid models are heuristically useful to understanding rostral biomechanics and generating testable hypotheses. Like other long-snouted mammals, the pig's rostrum forms a cylindrical, thin-walled shape that is probably best modeled as a hollow tube or beam. Hollow beam models have been used in structural analyses of the rostrum (Preuschoft et al., 1985; Thomason and Russell, 1986). Cylinder models have been used to predict/explain strain patterns not only in the mandible (Hylander, 1979), but also in the posterior parts of the cranium, specifically the hafting region (Greaves, 1985; Ross, 2001) and the braincase (Herring and Teng, 2000). In Greaves' model for the hafting region, the asymmetrical upward reaction forces at the bite point and contralateral jaw joint cause torsional loading of the skull during mastication. This torsion predicts the polarities and orientations of strain in the postorbital bar (Greaves, 1985). These predictions have received mixed support in experimental strain gauge studies (Hylander et al., 1991; Ross and Hylander, 1996; Ravosa et al., 2000; Ross, 2001). In the braincase region, forces from diagonal muscle couples (masseter and contralateral temporalis) set up torsion, producing predictable 45° strain orientations in the frontal and parietal bones (Herring and Teng, 2000). A cylinder model under torsion can also be used to predict strains in the rostral region (Fig. 1A). According to this model, a unilateral bite producing upward force anteriorly and masseter muscle contraction producing a downward force posteriorly will torque the rostrum. If the rostrum acts like a cylinder under torsion, the principal strains will have equal or similar magnitudes that lie at 45° to the long axis (Hylander, 1979; Hylander and Johnson, 1997). Furthermore, torsion will cause the principal strains on opposite sides of the cylinder to have opposite 45° orientations.

The rostrum can also be thought of as a fixed cylindrical beam subjected to upward forces at various locations along its length (corresponding to the teeth) (Fig. 1). The stresses and strains in the rostrum resulting from masticatory forces are likely to depend largely on its length and the point(s) of application of occlusal force. A long beam (length greater than three times the span) with a distally applied force will distort from bending (Fig. 1B). However, shearing deflections are more important in short beams (Roark and Young, 1982) (Fig. 1C). In a study on primates, Ross (2001) hypothesized that the interorbital region would behave like a short beam during mastication and more like a long beam during incisor biting.

In our previous work on miniature pigs, *Sus scrofa*, we suggested a long-beam bending model (Herring et al., 2001) because of a pattern of compression in the nasal sutures (Rafferty and Herring, 1999), but the 45° tensile strains observed in the maxilla are actually more consistent with the shear deformation model (Fig. 1C). In fact, at the level of the molariform teeth, the pig snout has a length/span ratio of about 0.6 to 1.8, with 1.0 for the mid-point of the toothrow, suggesting that the rostrum in this region should respond like a short beam. In the present study we provide a larger context for understanding rostral loading through the use of rosette strain gauges on the nasal and premaxillary bones as well as single element gauges on strategic sutures.

MATERIALS AND METHODS

The Hanford miniature strain of pigs, *Sus scrofa* (Charles River, Wilmington, MA), were used for the experiments. Sample sizes varied from 3–9, depending on location and procedure (see tables). The animals were 4–5 months old and included both sexes. All experimental procedures were approved by the Animal Care Committee of the University of Washington. Different animals had strain gauges applied to one or more locations on the premaxilla, nasal bone, maxillary-premaxillary suture, intermaxillary (palatal) suture, and internasal suture (Fig. 2).

Single element gauges (EP-08-125BT-120, Measurements Group, Raleigh, NC) were used to span the sutures, whereas the other locations received rosette gauges (SK-06-030WR-120).

The animals were anesthetized with halothane and nitrous oxide. A 4–5 cm skin incision was made along the crest that separates the dorsal from the lateral planes of the rostrum. The facial muscles running to the snout and lips were gently pushed laterally to expose the bone. With perpendicular relief incisions, this approach also allowed exposure of the nasal location. After elevating the periosteum the exposed bone was prepared and the strain gauges glued down as described previously (Rafferty and Herring, 1999; Rafferty et al., 2000). A thin strip of Teflon was placed along the suture in order to prevent glue from penetrating the suture space and adhering the margins when the gauge was placed. After testing the gauges for balance, the gauge orientation was measured and the periosteum and skin were separately sutured. A topical anesthetic (2% procaine hydrochloride) was drizzled on the incision and an analgesic (ketorolac tromethamine and/or buprenorphine hydrochloride) was given by i.m. injection prior to the recording session.

Fine-wire EMG electrodes were placed in the bilateral masseter and temporalis or zygomaticomandibularis muscles. The animals were allowed to awaken and were offered water and their normal diet of pig chow. The animals fed unrestrained and the amplified EMG and strain signals were digitized at 500 or 1,000 Hz on a Power MacIntosh running Acqknowledge III (Biopac Systems, Santa Barbara, CA). The relative onset and duration of muscle activity obtained from the EMG data allowed identification of the working vs. balancing sides during mastication (Huang et al., 1993). For the purpose of clarity, we will adopt the terminology ipsilateral to indicate when the working side was on the same side as the strain gauge and contralateral when it was on the opposite side. In two cases (8-6-98 and 8-7-98) EMG was not of adequate quality to determine chewing side, and in these cases all cycles were averaged together. The precise location of bite force application during mastication could not be ascertained.

After feeding, the animals were reanesthetized for the second phase of the procedure, in which strains were recorded in response to muscle stimulations. In four animals, an additional surgery was carried out to place a single element gauge across the intermaxillary suture. A tracheotomy was performed on these animals so that the oral cavity could be accessed without compromising anesthetic delivery. Only stimulation data are available for the intermaxillary suture because of the more invasive nature of this procedure.

All animals had needle electrodes placed posterosuperiorly and anteroinferiorly into the masseter on both sides. Tetani were produced by 400–600 msec trains of 3–5 msec pulses delivered at 60 pps (Model S48 and SIU, Grass Instrument Co., Quincy, MA). Strain data were recorded as the stimulation voltages were ramped up during a series of bilateral tetani to determine the appropriate level for supramaximal masseter contractions (usually 30–50 V). Both bilateral and unilateral contractions were produced with the molar teeth in occlusion. Because we were interested in the effect of forces at the teeth on patterns of strain in the rostrum, we also performed stimulations in some animals with a 6-mm-thick bite block, constructed of tongue depressors, placed between the incisors. After muscle stimulation, the animals were euthanized by intracardiac injection of pentabarbitol.

Chewing sequences were selected for analysis with the criteria that the animals were fully awake and were eating vigorously. Chewing sequences that included at least 10 consecutive chews were selected when possible. After identifying the working and balancing sides using the timing of the bilateral masseters and zygomaticomandibularis muscles, the wave data were resampled at 300 Hz in Acqknowledge and exported to Excel. After subtracting the baseline and converting to microstrain, the principal strains and angles were calculated. The maximum

principal strain, ε_{MAX}, is usually a positive value (tension) and the minimum principal strain, ε_{MIN}, is usually a negative value (compression). A similar procedure was carried out for the muscle stimulation data, except that mean values rather than raw waveform data were extracted. Data from multiple gauges on an individual were taken from the same chewing and stimulation sequences. Peak principal strains were selected based on the largest maximum shear strain, γ-max, which equals ε_{MAX} minus ε_{MIN}. Note that shear strain does not imply shear deformation; rather, it serves as a rough quantification of total strain magnitude. Descriptive statistics were calculated for ipsilateral and contralateral ε_{MAX}, ε_{MIN}, and ε_{MAX} orientation (ε_{MIN} orientation in the case of the nasal bones). Paired *t*-tests were used to compare ipsilateral and contralateral strains and orientations. A Friedman test (nonparametric analysis of variance) was used for ipsilateral, contralateral, and bilateral stimulation comparisons. A significance level of 0.05 was used.

RESULTS

Strains recorded during mastication are reported in Table 1 and Table 3 and Figure 3A and Figure 4A. Strains recorded during masseter muscle stimulation are reported in Table 2 and Table 4 and Figure 3B and Figure 4B.

Premaxillary Bones

Masticatory strains in the premaxilla were low (Table 1, Fig. 3A). The mean maximum shear strain (γ-max) was only 130 ± 55 με when pigs were chewing on the gauge (ipsilateral) side and 98 ± 32 με when they were chewing on the nongauge (contralateral) side (not significant, paired *t*-test). In two animals the premaxilla was in tension in both principal strain directions when they were chewing ipsilaterally. Tension was significantly greater for ipsilateral vs. contralateral side-chewing and compression was significantly greater (absolute magnitude) for contralateral vs. ipsilateral chewing side (Table 1). Differences between chewing sides were also highly significant for strain angle. When the pig was chewing on the same side as the gauge, the angle was rostrodorsally directed, but this angle became caudodorsal when the pig switched to the contralateral side (Fig. 3A).

Premaxillary strain recorded during masseter stimulation (Table 2, Fig. 3B) was similar in magnitude and direction to that recorded during mastication (Table 1, Fig. 3A). The magnitudes of strain (ε_{MAX}, ε_{MIN}, and γ-max) in the premaxillary rosette were not significantly different during ipsilateral, contralateral and bilateral masseter stimulation. The mean shear strain of all three stimulation modes was 140 ± 26 με. However, the strain angle changed dramatically according to the side of muscle activation. Ipsilateral and bilateral stimulation produced rostrodorsally directed maximum principal strain angles (67° ± 27 and 65° ± 33, respectively), whereas contralateral stimulation caused this angle to become caudodorsal (135° ± 29) (Table 2, Fig. 3B). This change in strain orientation was statistically significant (Friedman ANOVA, $P = 0.05$) and recalls that observed during chewing on the ipsilateral vs. contralateral sides, despite the fact that the masseter muscles are bilaterally active during mastication. Also, the ratios of εMAX/εMIN followed the trend observed in mastication: tension decreased relative to compression during contralateral stimulation (and mastication).

Nasal Bones

Masticatory strains measured from rosette gauges on the nasal bones (Table 1, Fig. 4A) were quite low in magnitude (66 ± 17 με and 84 ± 8 με mean shear strain for ipsilateral and contralateral cycles, respectively). Overall, compression was the dominant strain pattern on the nasal bones (Fig. 4A). While there were no significant differences between sides in strain magnitude (εMAX, εMIN, and γ-max) or orientation, compression increased in each animal when it chewed contralaterally and in two individuals both principal strains became

compressive. The average angle from the sagittal plane to the minimum compressive strain (β) was 105 ± 7.9°, indicating that the main axis of compression was roughly orthogonal to the internasal suture.

As with mastication, nasal strain during masseter stimulation was predominantly compressive, with the majority of animals showing biaxial compression (Table 2). There were no significant differences in strain magnitude between ipsilateral, contralateral, and bilateral stimulations. The mean shear strain for the three stimulations was 156 ± 115 με. The angle from the minimum principal strain to the internasal suture was caudolateral and varied little between the three modes of stimulation (mean 137 ± 7°). In four animals bilateral masseter stimulation was performed with and without an incisor bite block. Only one of the four showed biaxial nasal compression without the incisor bite, whereas all animals showed biaxial compression with the incisor bite as well as greatly increased absolute strains (data not shown).

Sutures

Compared to the strains on the surface of the premaxillary, nasal, and maxillary bones (Herring et al., 2001), the strains from the intervening sutures were larger by about an order of magnitude (Fig. 3, Fig. 4; Table 3). The maxillary–premaxillary suture on the lateral surface of the rostrum was always strongly tensed during mastication (Table 3, Fig. 3A). There were no significant differences in overall magnitude between chewing sides, although three out of the four animals did show larger strains when chewing ipsilaterally. The mean was 1,154 ± 462 με during mastication. The maxillary–premaxillary suture was also always in tension during masseter muscle stimulation (Table 4, Fig. 3B). Contralateral stimulation produced lower mean strains (528 ± 270 με) than ipsilateral and bilateral stimulation, (1,146 ± 890 με and 1,010 ± 667 με, respectively) but these differences were not significant.

Although we only measured internasal suture strains from three animals, all showed compression during mastication and bilateral masseter stimulation (−537 ± 187 με and −407 ± 286 με) (Table 3, Table 4; Fig. 4). This result is consistent with the previous finding of compression from more caudal locations of the internasal suture (Rafferty and Herring, 1999). In contrast, the intermaxillary suture (stimulation only) was strongly tensed during bilateral masseter stimulation (1,106 ± 571 με) (Table 4, Fig. 4). One would expect that the midline internasal and intermaxillary sutures would show the same patterns when only one masseter was stimulated. While this was usually the case, occasionally the strain polarity was opposite (small tension in the internasal and small compression in the intermaxillary during stimulation of one masseter but not the other). These polarity switches explain the large standard deviations in suture strains for unilateral stimulation in some individuals (Table 4). In addition to occasionally causing polarity switches, unilateral stimulation was also frequently associated with unstable baselines and movement artifacts in the suture waveforms (represented as “no data” in Table 4). These problems are a consequence of the asymmetrical movements caused by one-sided muscle contraction. Notably, bilateral stimulations faithfully reproduced strain patterns in the internasal and premaxillary–maxillary sutures observed during mastication.

DISCUSSION

Mechanical Role of Sutures

Although many of our findings may pertain to the unique craniofacial biomechanics of the pig, there are several general themes that are relevant in a broad sense of craniofacial biomechanics. One of the major findings of this study is that the bones of the pig rostrum do not experience large functional strains during mastication of pig chow. However, strains in facial sutures are much larger, often by an order of magnitude, than strains in facial bones. Previously, large

deformations have been recorded from braincase and other sutures (Herring and Mucci, 1991; Rafferty and Herring, 1999; Herring and Teng, 2000). The large disparity between strain magnitudes in braincase sutures and adjacent bones likely diminishes with maturity and suture fusion. In contrast, the facial sutures remain patent much longer, and as these compliant interfaces allow greater deformation than adjacent bony surfaces, they may protect the thin bones of the face during dynamic loading.

Based on strain recordings from the facial bones of cats (dry skulls and anesthetized animals), Buckland-Wright (1978) proposed that soft tissues in sutures absorb loads and in particular may protect the facial bones from overstress in response to large biting forces. More recently, Jaslow and Biewener (1995) measured large strain magnitudes in the cranial sutures of goats during in vitro impact loading. The observation that principal strains decreased dramatically from the frontal to parietal bone emphasizes the importance of the intervening suture as a shock absorber during impact (Jaslow and Biewener, 1995). The principle of shock absorption is only relevant for loads that occur over very short time intervals (as during mastication and impact loading) and not for static loads. The idea that the sutures of the face function as “strain sinks,” preventing the adjacent bony surfaces from large dynamic strains and allowing the bones to stay thin and light, ties in well with the overall mode of bone growth in the facial region. In the cranium, the largest functional strains occur at sutures *and* the majority of growth occurs at sutures. The large distortions in the sutures may stimulate osteogenesis at the interfaces.

Biomechanics of the Pig Rostrum

The reaction force produced at the cheek teeth is transmitted to the maxilla. Our previous work on the pig maxilla (Herring et al., 2001) can be summarized in the following points. 1) Maximum shear strains (γ-max) in the maxilla were on the order of 300 με and the magnitude of tension exceeded that of compression. 2) The angle of tension was directed rostrodorsally in all locations studied (see Fig. 2 and 3) Chewing strains in the maxilla were similar on the ipsilateral and contralateral sides but were larger than strains produced during supramaximal masseter stimulation.

Because the major load on the rostrum is occlusal force applied to the cheek teeth, it is reasonable that strains in the maxilla should be generally larger than those of the nasal and premaxillary bones during mastication, just as squamosal and condylar strains, which are close to applied muscle and joint loads, are greater than those of the more distant braincase (Herring and Teng, 2000; Herring et al., 2001). The fact that chewing strains in the maxilla were actually larger than strains produced during supramaximal masseter stimulation (Herring et al., 2001) reinforces the current findings on the premaxillary bone and the maxillary–premaxillary and internasal sutures in implicating occlusal loading as an important factor in rostral strain. In posterior regions from which we have measured strain (zygomatic arch, condyle, braincase), muscle stimulation produces similar patterns and similar or higher magnitudes of strain than mastication (Herring and Mucci, 1991; Herring et al., 1996; Marks et al., 1997; Herring and Teng, 2000; Rafferty et al., 2000). On the snout, the importance of occlusal force is increased and that of masseter contraction diminished. In contrast to masseter stimulation, the activity of mastication uses several muscles in controlled patterns of activation to produce a precise and forceful occlusion. Thus, the higher masticatory strains observed in the maxilla probably reflect better occlusal contact, if not larger bite forces, than occur during muscle stimulation.

Except for the premaxillary bones (see below), no differences in strain patterns were observed in association with chewing side in any rostral location. This surprising finding probably reflects the fact that pigs have isognathic tooth rows and molar contact is likely bilateral (Herring et al., 2001). In dry pig skulls it is virtually impossible to occlude one tooth row to the exclusion of the other. In terms of magnitude, pigs also have similar strains on the working and balancing side mandibular corpus and condyle (Liu and Herring, 2000) and zygomatic

arch (Rafferty et al., 2000). A combination of a bilateral bite and similar amounts of balancing and working side muscle recruitment means that the forces are similar on both sides. As an anisognathic artiodactyl, sheep provide the most relevant available comparison to pigs (Thomason et al., 2001). Maxillary strain on the contralateral (balancing) side in sheep was highly tensile and oriented dorsoventrally, reflecting the pull of the masseter on that side (and a lack of an occlusal force) (Thomason et al., 2001). In contrast, the ipsilateral (working) side strains showed slightly larger compression than tension, with tension oriented rostrodorsally, reflecting primarily the bite force (Thomason et al., 2001). The rostrodorsal orientation of tension on the ipsilateral side is quite similar in orientation to that seen on both sides in pigs (Herring et al., 2001). At least in this respect, the two sides in pigs resemble the ipsilateral side of sheep, lending credence to the idea that both sides in pigs are the ipsilateral side (in terms of occlusal contact but not jaw movement).

The torsion model of the rostrum (Fig. 1A) requires a unilateral bite force and predicts alternating 45° rostrodorsal and caudodorsal tensile orient ations in association with working and balancing sides. This model may be appropriate for sheep, but it clearly can be rejected for the pig rostrum. The maxillary strains of the pig are more consistent with the model of the rostrum as a short beam under shear deformation (Fig. 1C). The tapered structure of the rostrum in pigs and other mammals violates the assumption of a uniform cross-section in the analysis of beams (Roark and Young, 1982). This anteroposterior change in cross-sectional shape along the rostrum has the effect of equalizing the shear stresses from the teeth along the length of the upper jaw (Preuschoft et al., 1985). The similar strains in anterior, middle, and posterior locations of the maxilla support the notion that this part of the rostrum is a “body of equal strength against the shearing forces” (Preuschoft et al., 1985:1).

Alone among the locations studied, the premaxilla had distinctly different ipsilateral and contralateral side strain pattern consistent with torsion (Fig. 1A). The ipsilateral strain pattern was similar to the pattern in the adjacent maxilla during mastication. Tension was much larger than compression and was oriented rostrodorsally. In contrast, the strain angle shifted to rostrocaudal and compression increased during contralateral mastication (side opposite to premaxillary gauge). The two animals with biaxial tension switched to a pattern of tensile and compressive principal strains. We speculate that these patterns arise from incisor contact as the mandible swings away from or towards the gauge side, respectively, at the end of the power stroke (Fig. 5). Unlike the cheek teeth, the incisors do not have broad contact, but meet at one point at a time. The alternating contacts during ipsilateral and contralateral chewing must twist the premaxillae in opposite directions, accounting for the large shift in the orientation of the tensile axis. In addition to torsion, the increased tension on the ipsilateral side and increased compression on the contralateral side indicate bending in the transverse plane (Fig. 5). Unilateral masseter stimulation recreates the same jaw movement as mastication (ipsilateral stimulation causes the jaw to move to the contralateral side and vice versa) and hence the same strain patterns.

As expected from the short-beam model, the maxillary–premaxillary suture is tensed during both mastication and muscle stimulation. The uni-axial gauge used does not show the exact orientation of this tension and, in fact, shear and convex bending will also be recorded as tension (Herring and Rafferty, 2000). However, the rostrodorsal orientation of tension in the maxilla is consistent with simple tension across the maxillary–premaxillary suture. The torsion/transverse bending strain pattern in the premaxilla during contralateral side mastication / contralateral muscle stimulation can be detected as a tendency for decreased tensile strain (Table 3, Table 4; Fig. 3).

Although the long beam model predicts longitudinal compression in the nasal bones, the observed compressive strains were mainly transverse, even when biaxial compression

occurred. The compressive strain pattern is also seen in the internasal suture. None of the models presented in Figure 1 explain this striking finding. However, in combination with the strong transverse tension shown by the intermaxillary suture during masseter stimulation, and possibly during mastication, an additional loading pattern is revealed (Fig. 6). The bilateral loading from the occluding cheek teeth in pigs deforms the rostrum, causing the two maxillae to pull apart slightly on the ventral surface at the intermaxillary suture and pushing the nasal bones together on the dorsal surface at the internasal suture (Fig. 6). In this scenario, we would expect that the maxillary–nasal suture would be compressed. Unfortunately, these two bones meet at a near right angle, making it impossible to obtain strain data.

In retrospect, long-beam bending of the rostrum due to incisor loading (Fig. 1) probably would be difficult to detect, because in pigs the incisors cannot occlude without the molars also being in occlusion. Thus, the short-beam shearing model is always prominent. Nevertheless, a tendency for long-beam bending deformation may be indicated by the frequent biaxial compression in the nasal bones, suggesting a complex pattern of loading in which upward bending is superimposed on lateral compression. Support for this comes from the finding that an anterior bite block during stimulation greatly increased the biaxial compressive strains.

CONCLUSIONS

During mastication, the premaxillary and nasal bones of pigs experience much lower magnitudes of strain than the nearby maxillary–premaxillary and internasal sutures. The large deformation in these and other sutures may be important in limiting the strain that can develop in the delicate bones of the face during dynamic loading. In addition, the fact that considerable strains are focused at sutural margins is consistent with an interpretation of mechanically regulated osteogenesis at these major growth sites. Despite the disparity in strain between bones and sutures, there is evidence that the rostrum behaves mechanically like a solid structure under simple forms of loading. In particular, strain in the maxilla was consistent with a short beam model of ventrodorsal shear from the cheek teeth. There was no evidence for torsion of the posterior rostrum, a finding that is easily explained by the bilateral occlusal contact in pigs. Torsional loading of the maxilla is likely to be common in other long-snouted mammals, most of which have unilateral occlusion. The premaxilla was the only bone to demonstrate working and balancing side differences in strain pattern that were consistent with torsional loading. These differences are attributed to asymmetrical incisor contact occurring at the end of the power stroke. Beam models did not account for all of the strain patterns observed. In the mediolateral plane there is evidence that the two halves of the hard palate pull apart at the intermaxillary suture and the nasal bones push together at the internasal suture. The unusual pattern of biaxial compression of the nasal bones suggests a complex pattern of loading in which lateral compression of the nasals is superimposed on upward bending.

Acknowledgments

We thank Pannee Ochareon and Zongyang Sun for assistance with experiments.

Contract grant sponsor: the National Institute of Dental Research; Contract grant number: PHS grant DE08513.

LITERATURE CITED

Buckland-Wright JC. Bone structure and the patterns of force transmission in the cat skull (*Felis catus*). J Morphol 1978;155:35–62. [PubMed: 619163]

Demes, B.; Preuschoft, H.; Wolff, JEA. Food acquisition and processing in primates. Chivers, DJ.; Wood, BA.; Bilsborough, A., editors. New York: Plenum Press; 1984. p. 369-390.

Greaves WS. The mammalian postorbital bar as a torsion-resisting helical strut. J Zool (A) 1985;207:125–136.

Herring SW, Mucci RJ. In vivo strain in cranial sutures: the zygomatic arch. J Morphol 1991;207:225–239. [PubMed: 1856873]

Herring, SW.; Rafferty, KL. Cranial and facial sutures: functional loading in relation to growth and morphology. In: Davidovitch, Z.; Mah, J., editors. Biological mechanisms of tooth eruption, resorption and replacement by implants. Boston: Harvard Society for Advanced Orthodontics; 2000. p. 269-276.

Herring SW, Teng S. Strain in the braincase and its sutures during function. Am J Phys Anthropol 2000;112:575–593. [PubMed: 10918130]

Herring SW, Teng S, Huang X, Mucci RJ, Freeman J. Patterns of bone strain in the zygomatic arch. Anat Rec 1996;246:446–457. [PubMed: 8955784]

Herring SW, Rafferty KL, Liu ZJ, Marshall CD. Jaw muscles and the skull in mammals: the biomechanics of mastication. Comp Biochem Physiol Part 1 2001;31:207–219.

Huang X, Zhang G, Herring SW. Alterations of muscle activities and jaw movements after blocking individual closing muscles in the miniature pig. Arch Oral Biol 1993;38:291–297. [PubMed: 8517800]

Hylander WL. Mandibular function in *Galago crassicaudatus* and *Macaca fascicularis*: an in vivo approach to stress analysis of the mandible. J Morphol 1979;159:253–296. [PubMed: 105147]

Hylander WL. Stress and strain in the mandibular symphysis of primates: A test of competing hypotheses. Am J Phys Anthropol 1984;64:1–46. [PubMed: 6731608]

Hylander WL. Mandibular function and biomechanical stress and scaling. Am Zool 1985;25:315–330.

Hylander WL, Johnson KR. Jaw muscle function and wish-boning of the mandible during mastication in macaques and baboons. Am J Phys Anthropol 1994;94:523–547. [PubMed: 7977678]

Hylander WL, Johnson KR. In vivo bone strain patterns in the zygomatic arch of macaques and the significance of these patterns for functional interpretations of craniofacial form. Am J Phys Anthropol 1997;102:203–232. [PubMed: 9066901]

Hylander WL, Picq P, Johnson KR. Masticatory-stress hypotheses and the supraorbital region of primates. Am J Phys Anthropol 1991;86:1–36. [PubMed: 1951658]

Jaslow CR. Mechanical properties of cranial sutures. J Biomech 1990;23:313–321. [PubMed: 2335529]

Jaslow CR, Biewener AA. Strain patterns in the horncores, cranial bones and sutures of goats (*Capra hircus*) during impact loading. J Zool Lond 1995;235:193–210.

Liu ZJ, Herring SW. Masticatory strains on osseous and ligamentous components of the jaw joint in miniature pigs. J Orofacial Pain 2000;14:265–278. [PubMed: 11203760]

Marks L, Teng S, Årtun J, Herring S. Reaction strains on the condylar neck during mastication and maximum muscle stimulation in different condylar positions: an experimental study in the miniature pig. J Dent Res 1997;76:1412–1420. [PubMed: 9207775]

Preuschoft H, Demes B, Meier M, Bär HF. Die biiomechanischen Prinzipien im Oberkiefer von langschnauzigen Wirbeltieren. Z Morph Anthrop 1985;76:1–24.

Rafferty KL, Herring SW. Craniofacial sutures: morphology, growth and in vivo masticatory strains. J Morphol 1999;242:167–179. [PubMed: 10521876]

Rafferty KL, Herring SW, Artese F. Three-dimensional loading and growth of the zygomatic arch. J Exp Biol 2000;203:2093–3004. [PubMed: 10862722]

Ravosa MJ, Johnson KR, Hylander WL. Strain in the galago facial skull. J Morphol 2000;245:51–66. [PubMed: 10861831]

Roark, RJ.; Young, WC. Formulas for stress and strain. New York: McGraw-Hill; 1982.

Ross CF. In vivo function of the craniofacial haft: the interorbital “pillar.”. Am J Phys Anthropol 2001;116:108–139. [PubMed: 11590585]

Ross CF, Hylander WL. In vivo and in vitro bone strain in the owl monkey circumorbital region and the function of the postorbital septum. Am J Phys Anthropol 1996;101:183–215. [PubMed: 8893085]

Thomason JJ, Russell AP. Mechanical factors in the evolution of the mammalian secondary palate: a theoretical analysis. J Morphol 1986;189:199–213. [PubMed: 3746918]

Thomason JJ, Grovum LE, Deswysen AG, Bignell WW. In vivo surface strain and stereology of the frontal and maxillary bones of sheep: implications for the remodeling and mechanical optimization of cranial bones. Anat Rec 2001;264:325–338. [PubMed: 11745088]

van Eijden TMGJ. Biomechanics of the mandible. Crit Rev Oral Biol Med 2000;11:123–136. [PubMed: 10682903]

Wolff, JEA. A theoretical approach to solve the chin problem. In: Chivers, DJ.; Wood, BA.; Bilsborough, A., editors. Food acquisition and processing in primates. New York: Plenum Press; 1984. p. 391-405.

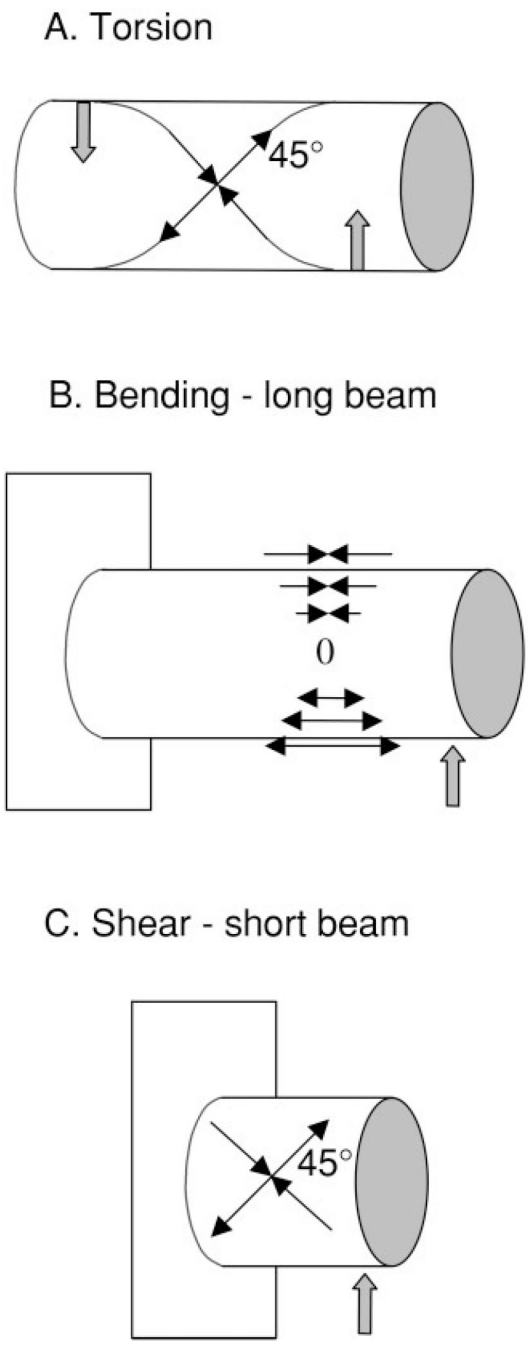

Fig. 1.

Cylinder models under torsion (**A**), bending (**B**), and shear (**C**). Solid upward arrows represent occlusal forces and the downward arrow (**A**) represents masseter muscle force. Thin arrows indicate tensile strain (arrows pointing out) and compressive strain (arrows pointing in). See text for further explanation.

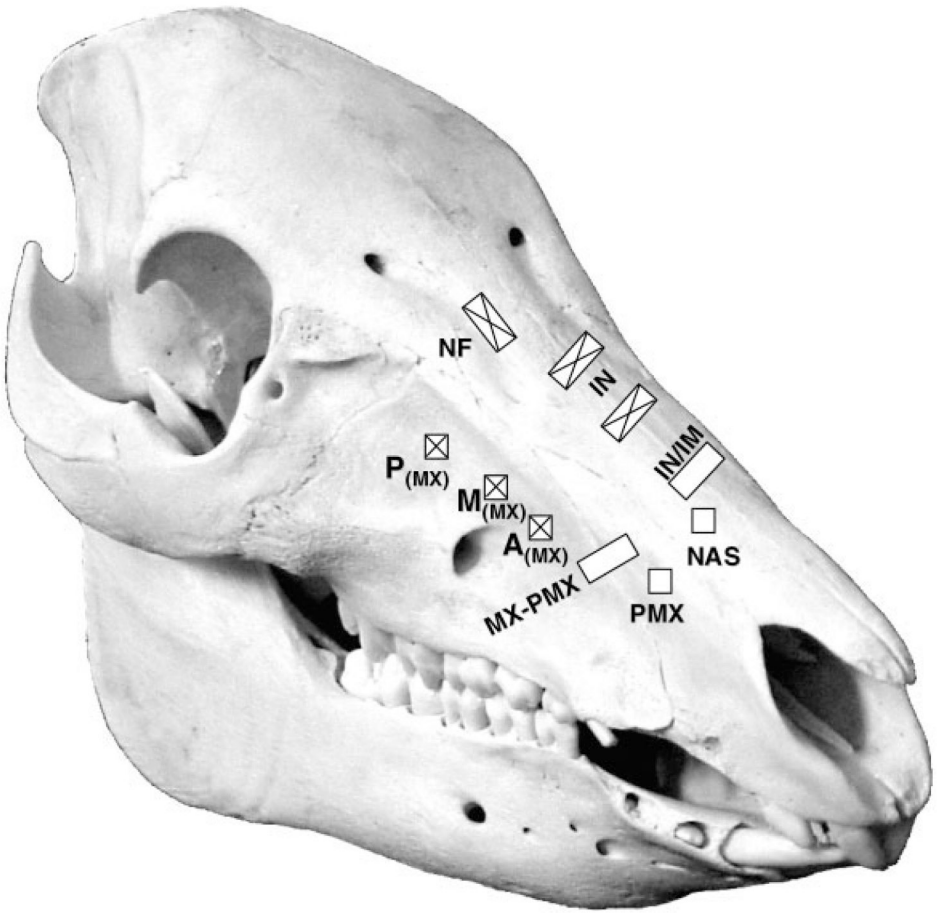

Fig. 2.

Sus scrofa. Location of strain gauges in dorsolateral view. Squares represent rosettes and rectangles represent single element gauges. Gauges with crosses indicate published data reconsidered here (Herring et al., 2001; Rafferty and Herring, 1999). P(MX), M(MX), and A (MX) are posterior, middle, and anterior maxillary locations; PMX and NAS are premaxillary and nasal locations. MX-PMX, IN, IM, and NF are the maxillary–premaxillary, internasal, intermaxillary, and nasofrontal suture locations. The intermaxillary gauge is on the palate and cannot be seen in this view, but is labeled with the internasal suture because of its similar caudorostral location.

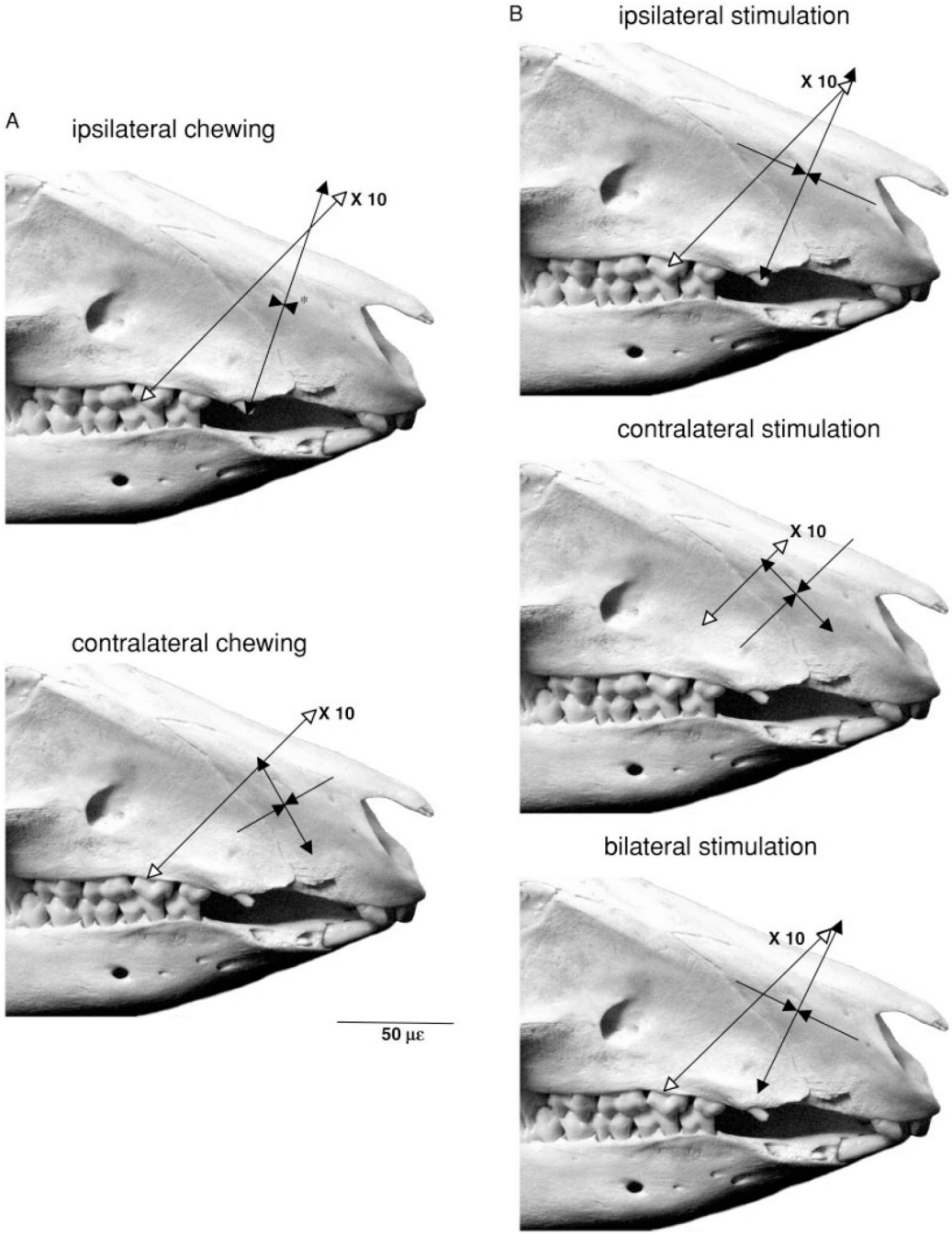

Fig. 3.

Sus scrofa. Average peak strains from single element gauges across the maxillary–premaxillary suture and average peak principal strains/orientations from rosette gauges on the premaxillary bone during (**A**) mastication and (**B**) masseter muscle stimulation. Tensile strains indicated by lines with arrows pointing in opposite directions and compressive strain by lines with converging arrows. Suture strains have open arrowheads and are 10 times their shown magnitude, as indicated by scale bar. The asterisks indicate that the arrowheads do not accurately reflect the small magnitude of the mean strain.

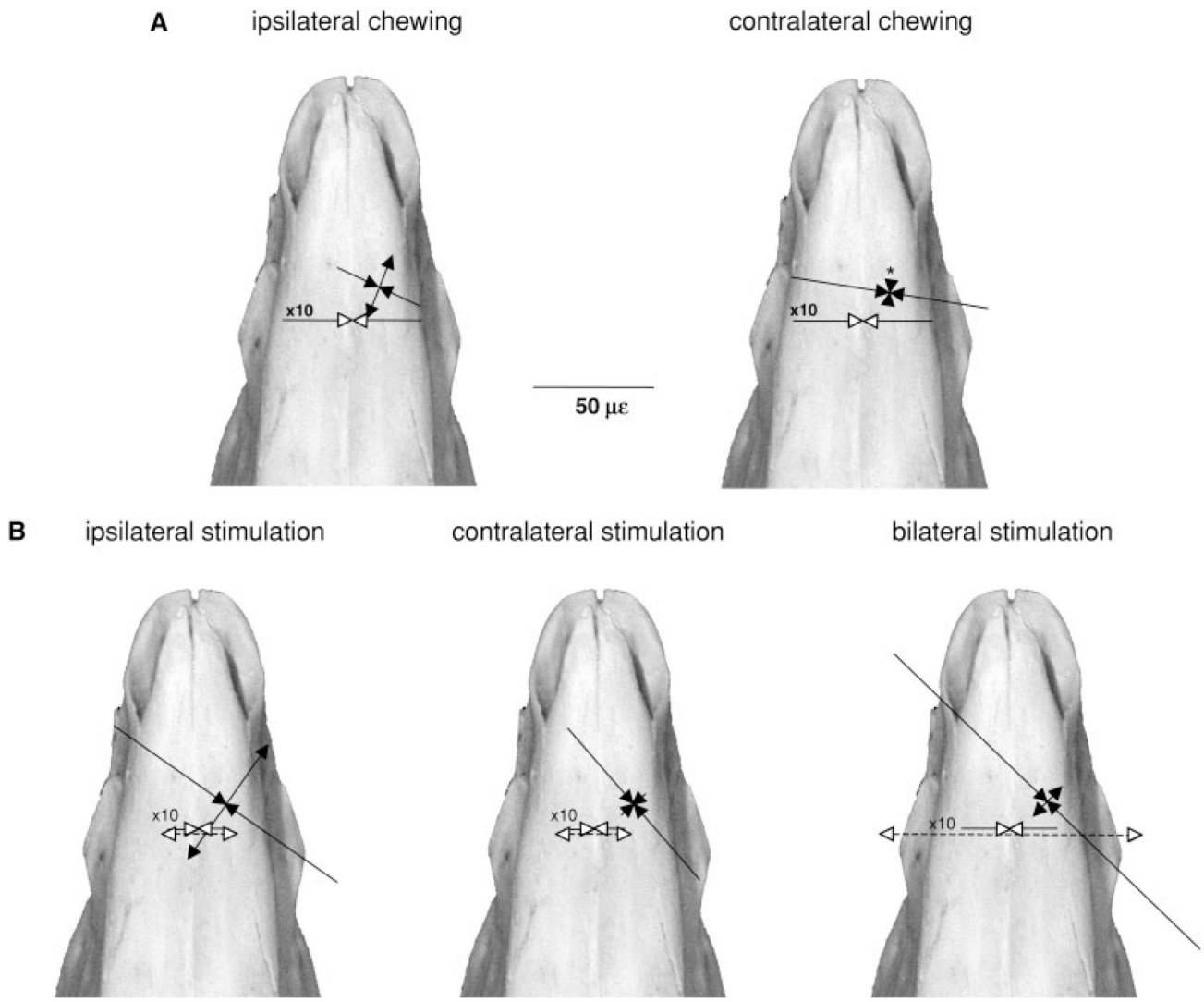

Fig. 4.

Sus scrofa. Average peak strains from single element gauges across the internasal suture (solid lines) and intermaxillary sutures (dotted lines) and average peak principal strains/orientations from rosette gauges on the nasal bone during (**A**) mastication and (**B**) masseter muscle stimulation. Tensile strains are indicated by lines with arrows pointing in opposite directions and compressive strains by lines with converging arrows. Suture strains have open arrowheads and are 10 times their shown magnitude, as indicated by scale bar. Right and left unilateral stimulation strains are averaged for the intermaxillary and internasal suture (see Table 4). The asterisk indicates that the compressive arrowheads do not accurately reflect the small magnitude of the mean compressive strain.

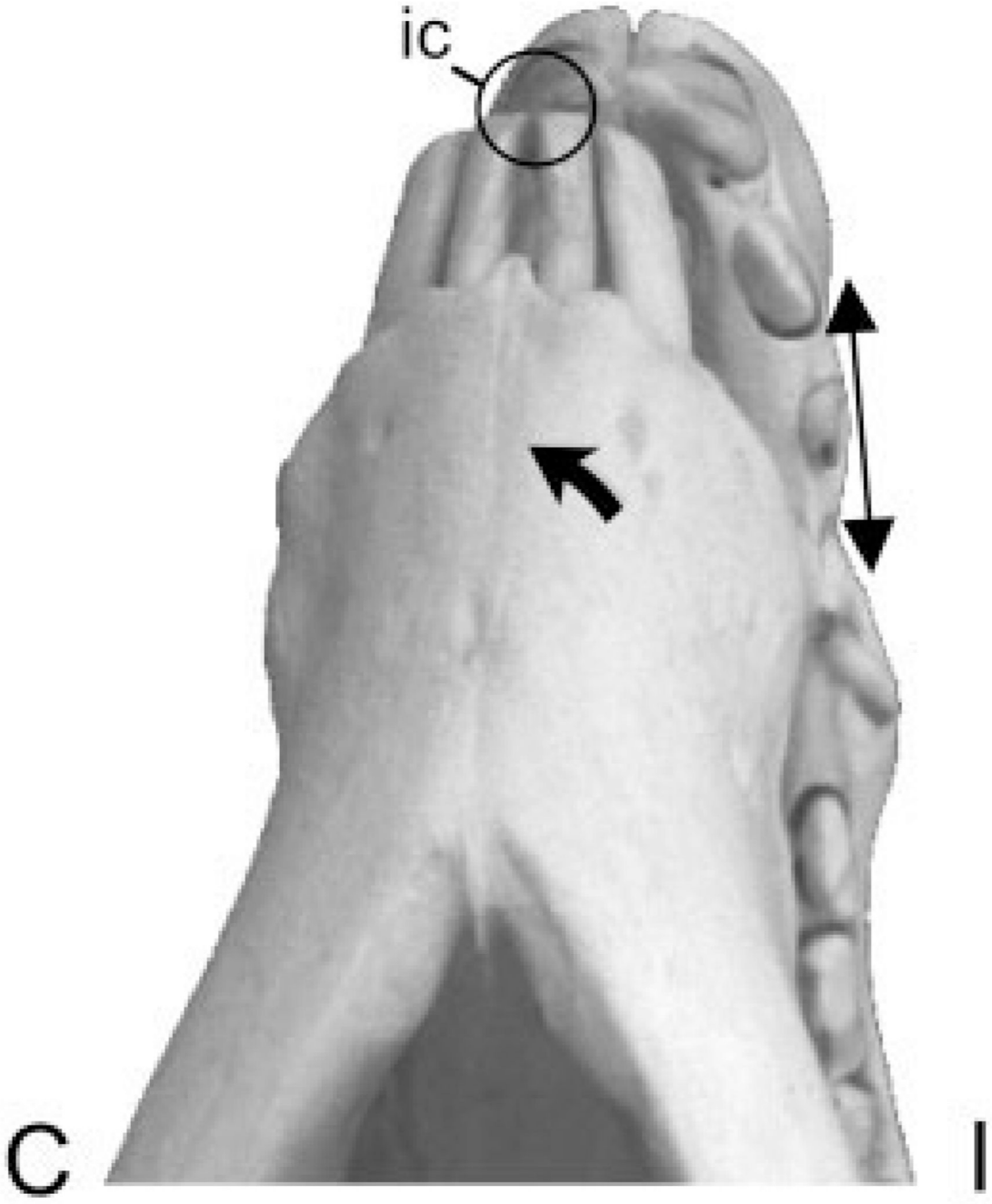

Fig. 5.

Sus scrofa. Ventral view of the mandible and rostrum showing incisor contact as the mandible swings away from the gauge side (ipsilateral, I) at the end of the power stroke. The large arrow indicates the direction of this movement. This asymmetrical incisor contact (ic) twists the premaxillary bones, resulting in tension (diverging arrows) on the ipsilateral premaxilla, while the contralateral premaxilla (C) is compressed (not shown).

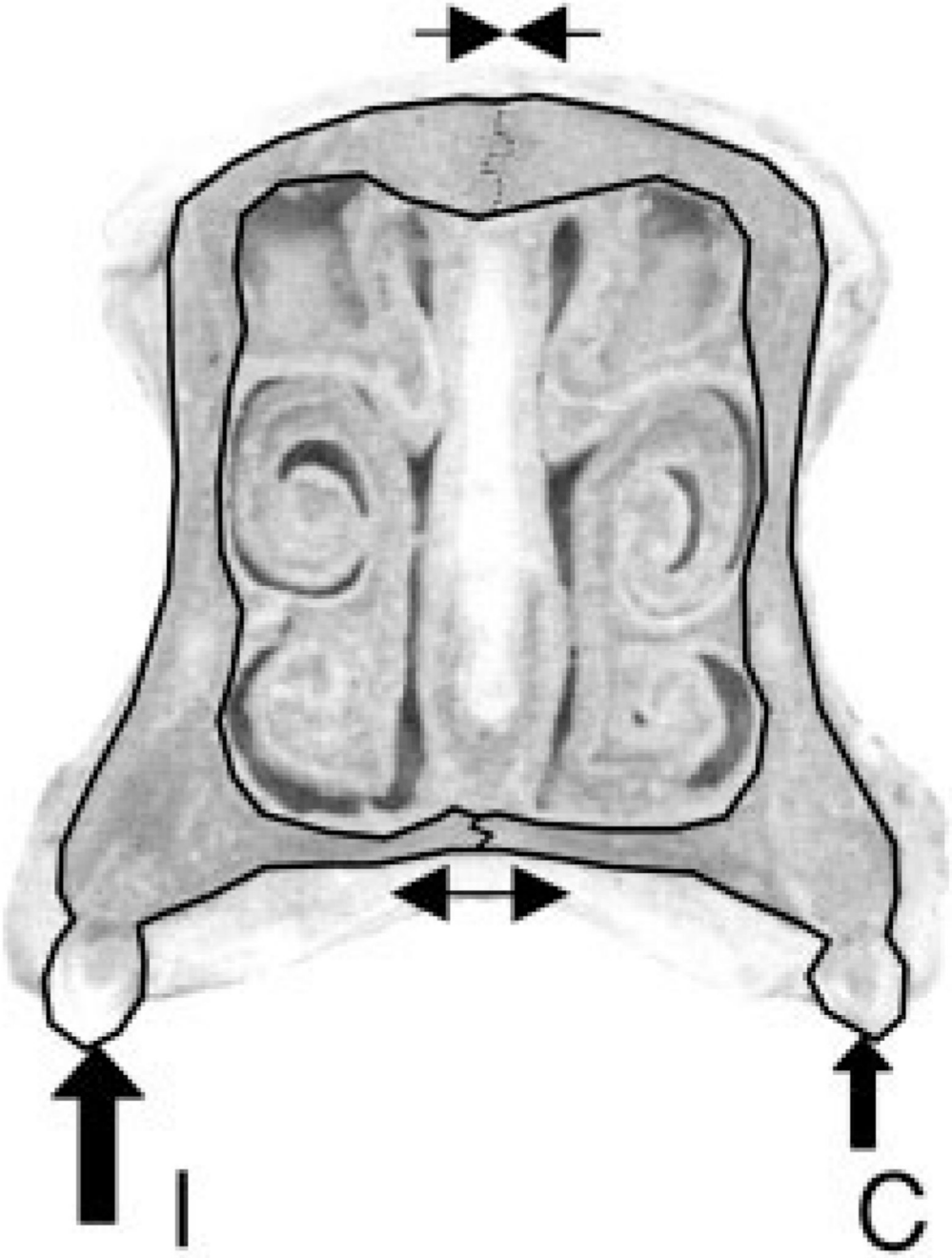

Fig. 6.

Sus scrofa. Interpretation of rostral loading and strain patterns in cross-sectional view. The cheek tooth force is applied bilaterally (solid arrows on ipsilateral, I, and contralateral, C, molars), causing compression of the internasal suture (line with converging arrows) and tension in the intermaxillary suture (line with opposite arrows).

J Morphol. Author manuscript; available in PMC 2010 February 10.

TABLE 1

Premaxillary and nasal bones: peak principal strains during mastication

	Premaxillary				*Nasal*			
ID no.	**Side (N)**	**ε_{MAX} (με)**	**ε_{MIN} (με)**	**α (degrees)**	**Side (N)**	**εMAX(με)**	**εMIN (με)**	**B (degrees)**
5-7-99	I (12)	91 (32)	−20 (10)	76 (15)				
	C (8)	34 (7)	−43 (13)	114 (8)				
8-3-00[a]	I (19)	157 (35)	−25 (6)	85 (3)	I (10)	78 (15)	−5 (7)	113 (13)
	C (18)	61 (36)	−41 (20)	108 (15)	C (10)	−16 (5)	−95 (17)	90 (5)
5-2-01	I (13)	75 (22)	−28 (16)	34 (4)	I (13)	12 (8)	−32 (12)	98 (6)
	C (15)	60 (18)	−71 (25)	132 (4)	C (15)	−11 (6)	−93 (20)	77 (3)
7-5-01					I (13)	12 (14)	−64 (25)	116 (5)
					C(14)	9 (15)	−69 (31)	115 (6)
9-20-01	I (10)	134 (37)	57 (29)	98 (7)				
	C (10)	33 (8)	−23 (12)	129 (3)				
9-26-01	I (16)	62 (21)	2 (15)	72 (22)	I (16)	12 (8)	−50 (14)	114 (3)
	C (16)	56 (16)	−69 (31)	115 (2)	C (16)	11 (5)	−84 (24)	116(2)
	I (5)	**104 (40)**	**−3 (35)**	**73 (24)**	**I (4)**	**29 (33)**	**−38 (26)**	**110 (8)**
	C (5)	**49 (14)***	**−49 (20)***	**120 (10)***	**C (4)**	**−2 (14)**	**−85 (12)**	**99 (20)**

Values are means (SD). Group means are bolded.

I, ipsilateral; C, contralateral; ε_{MAX}, peak tensile strain; ε_{MIN}, peak compressive strain; α, angle of maximum principal strain to occlusal plane (see Fig. 2); β, angle of minimum principal strain to internasal suture (see Fig. 3).

[a]Nasal strain data during mastication of pig chow were unavailable for this animal. Instead, data were collected when the animal was chewing on a plastic tube on the right side. Ipsilateral data are from the right side rosette, contralateral data are from the left side rosette.

*I and C significantly different, $P < 0.05$, paired *t*-tests.

TABLE 2

Premaxillary and nasal bones: principal strains during masseter stimulation

		Ipsilateral				Contralateral				Bilateral			
ID No.	**Gauge**	**N**	**ε_{MAX} (με)**	**ε_{MIN} (μ)**	**angle (degrees)**	**N**	**ε_{MAX} (με)**	**εMIN (με)**	**angle (degrees)**	**N**	**ε_{MAX} (με)**	**εMIN (με)**	**angle (degrees)**
5-7-99	PMX	5	56 (3)	−96 (3)	61 (0)	5	23 (1)	−99 (4)	146 (0)	5	−14 (6)	−110 (5)	INDETER
8-3-00	PMX	3	182 (5)	−105 (3)	83 (0)	5	76 (1)	−48 (1)	147 (0)	7	112 (2)	−99 (3)	75 (1)
5-2-01	PMX	4	54 (8)	−40 (6)	38 (4)	4	11 (0)	−8 (0)	85 (1)	4	30 (1)	−18 (2)	30 (4)
6-29-01	PMX	7	198 (9)	−133 (5)	29 (1)		NO DATA			7	168 (4)	−71 (2)	25 (0)
7-5-01	PMX	8	54 (11)	−12 (2)	75 (3)		NO DATA			8	131 (8)	−7 (2)	65 (1)
9-20-01	PMX	5	124 (6)	−59 (2)	76 (0)	5	51 (1)	−113 (3)	159 (0)	5	112 (7)	−34 (3)	85 (0)
9-26-01	PMX	5	37 (1)	−12 (1)	109 (1)	5	65 (1)	−73 (3)	136 (0)	5	52 (3)	−72 (3)	112 (0)
		7	**101 (67)**	**−65 (47)**	**67 (27)**	**5**	**45 (28)**	**−68 (42)**	**135 (29)***	**7**	**84 (64)**	**−59 (40)**	**65 (33)**
10-1-97	NAS	15	−11 (2)	−242 (8)	102 (3)	16	−64 (11)	−261 (18)	113 (3)	16	−12 (11)	−470 (25)	105 (2)
10-2-97	NAS	11	−12 (1)	−179 (6)	154 (1)	8	−13 (2)	−124 (2)	120 (1)	6	−70 (2)	−243 (2)	102 (1)
11-12-97	NAS	8	−27 (4)	−46 (3)	INDETER	8	−12 (2)	−31 (2)	113 (6)	8	−27 (2)	−78 (10)	168 (1)
11.10.97	NAS	8	−7 (1)	−63 (2)	171 (1)	8	−22 (3)	−45 (2)	125 (2)	8	−17 (1)	−116 (2)	161 (1)
8-3-00	NAS	5	268 (6)	−280 (6)	103 (0)	5	−10 (1)	−30 (1)	141 (5)	5	197 (17)	−278 (19)	95 (0)
5-2-01	NAS	4	197 (7)	−178 (5)	169 (1)	4	−6 (1)	−24 (1)	143 (2)	4	90 (1)	−78 (1)	165 (0)
6-29-01	NAS	4	57 (6)	−122 (2)	176 (1)		NO DATA				NO DATA		
7-5-01	NAS	8	75 (5)	−120 (7)	169 (1)	8	−6 (3)	−81 (7)	153 (0)	8	17 (2)	−74 (3)	158 (1)
9-26-01	NAS	5	−8 (2)	−50 (2)	114 (1)	5	14 (1)	−70 (3)	139 (0)	5	−37 (1)	−90 (4)	136 (1)
		9	**59 (106)**	**−115 (122)**	**145 (33)**	**8**	**−15 (22)**	**−83 (79)**	**131 (15)**	**8**	**18 (86)**	**−178 (142)**	**136 (31)**

Values are means (SD). Group means are bolded. PMX = premaxillary rosette gauge, NAS = nasal rosette gauge. Other abbreviations same as Table 1.

INDETER = angles are indeterminate due to similar values for the three gauge elements.

*Contralateral significantly different from ipsilateral and bilateral (Friedman test, $P \leq 0.05$).

TABLE 3

Peak sutural strains during mastication

	Maxillary-Premaxillary		Internasal	
ID no.	**Side (N)**	**MX-PMX (με)**	**Side (N)**	**IN (με)**
8-6-98			I/C (21)	−761 (224)
8-7-98			I/C (15)	−503 (38)
5-2-01	I (13)	1019 (127)		
	C (15)	649 (121)		
7-5-01	I (13)	710 (129)		
	C (14)	731 (143)		
9-20-01	I (10)	1393 (187)		
	C (10)	1298 (155)		
9-26-01	1 (15)	1966 (367)	I/C (31)	−445 (178)
	C (16)	1463 (212)		
	1 (4)	**1272 (540)**	**I/C (3)**	**−570 (168)**
	C (4)	**1035 (406)**		

Values are means, SD. Group means are bolded.

I, ipsilateral; C, contralateral; MX-PMX, maxillary-premaxillary suture; IN, internasal suture.

TABLE 4

Suture strains during masseter stimulation

	Maxillary-Premaxillary		Internasal		Intermaxillary	
ID no.	**Side (N)**	**Strain (με)**	**Side (N)**	**Strain (με)**	**Side (N)**	**Strain (με)**
11-10-97			I/C (30)	−451 (63)	I/C (nodata)	
			B (19)	−823(38)	B (17)	1014 (118)
11-12-97			I/C (nodata)		I/C (26)	411 (44)
			B (11)	−273(33)	B (11)	1276 (73)
5-2-01	I (4)	230 (48)				
	C (4)	56 (7)				
	B (4)	360 (42)				
6-29-01	I (7)	1470 (81)				
	C (8)	673 (75)				
	B (7)	1818 (132)				
7-5-01	I (nodata)					
	C (8)	560 (76)				
	B (8)	426 (42)				
8-24-01			I/C (18)	−221(19)	I/C (12)	778 (29)
			B (6)	−354(10)	B(6)	1916 (100)
9-20-01	I (5)	648 (211)			I/C (5)	98 (390)
	C (5)	709 (162)			B (5)	992 (22)
	B (5)	854 (108)				
9-26-01	I (5)	2234 (52)	I/C (10)	−107 (246)	I/C (10)	6 (112)
	C (5)	643 (74)	B (5)	−179 (35)	B (5)	332 (18)
	B (5)	1594 (86)				
	I (4)	**1146 (890)**	**I/C (3)**	**−260 (175)**	**I/C (4)**	**323 (234)**
	C (5)	**528 (270)**				
	B (5)	**1010 (667)**	**B (4)**	**−407 (286)**	**B (5)**	**1106 (571)**

Values are means (SD). Group means are bolded.

I, ipsilateral; C, contralateral; B, bilateral.